

Neural Network-Based Stabilizer for the Improvement of Power System Dynamic Performance

Rudy Gianto*, Kho Hie Khwee

Department of Electrical Engineering, Tanjungpura University, Jalan Prof. Dr. H. Hadari Nawawi,
Pontianak 78124, Indonesia

*Corresponding author, e-mail: rudygianto@gmail.com

Abstract

This paper develops an adaptive control coordination scheme for power system stabilizers (PSSs) to improve the oscillation damping and dynamic performance of interconnected multimachine power system. The scheme was based on the use of a neural network which identifies online the optimal controller parameters. The inputs to the neural network include the active- and reactive- power of the synchronous generators which represent the power loading on the system, and elements of the reduced nodal impedance matrix for representing the power system configuration. The outputs of the neural network were the parameters of the PSSs which lead to optimal oscillation damping for the prevailing system configuration and operating condition. For a representative power system, the neural network has been trained and tested for a wide range of credible operating conditions and contingencies. Both eigenvalue calculations and time-domain simulations were used in the testing and verification of the performance of the neural network-based stabilizer.

Keywords: neural network, PSS, dynamic performance, oscillation damping, power system

Copyright © 2017 Universitas Ahmad Dahlan. All rights reserved.

1. Introduction

Following the restructuring of the power supply industry and increased trend of interconnecting power systems, the damping of electromechanical modes of oscillations among the interconnected synchronous generators, including the inter-area modes, is a growing concern, and constitutes one of the essential criteria for secure system operation.

It has been acknowledged that PSSs can enhance or maintain the stability of the electromechanical modes and improve the dynamic performance of a power system. In this context, there has been extensive research in the application of PSSs, particularly their control coordination, for achieving optimal damping of electromechanical modes, including inter-area modes in a power system [1-7]. In [1-7], control coordination design procedures in off-line environments which lead to fixed-parameter controllers have been reported. However, it is, in general, accepted that there are disadvantages associated with fixed-parameter controllers, even with those obtained by robust design. If the design is based on one particular power system operating condition and configuration, it is possible that the performances of the controllers will deteriorate under other operating conditions or configurations.

With the objective of removing the disadvantages of fixed-parameter controllers, adaptive control techniques applied for power system damping controller design have been developed by some researchers [7-15]. In [7-13], artificial neural networks were proposed for implementing PSS in a single-machine infinite bus system. However, control coordination among different PSSs in multimachine power system was not considered in the papers. Furthermore, the changes in system configuration due to contingencies, which have a significant impact on electromechanical mode dampings, were not discussed in the design procedure. In [14], ANFIS-based PSSs have been proposed for improving the dynamic stability of a part of a power system (area that containing three synchronous machines). However, the performance of the stabilizer on larger multimachine power system was not discussed in the paper. Moreover, the stabilizer design proposed in [14] only dealt with the system load fluctuations. The changes in system configuration were not considered in the paper.

In [15], an adaptive and optimal control coordination scheme for power system damping controllers has been developed. Central to scheme proposed in [15] is the use of

neural network synthesized to give in its output layer the optimal controller parameters adaptive to system operating condition and configuration. Although, the control coordination scheme has successfully been applied in enhancing and maintaining stability of a small power system (system that containing four synchronous machines), its performance, however, on larger interconnected multi-machine power systems is still a problem and consequently needs to be addressed and investigated.

Therefore, against the above background, the objective of the present paper is to apply and extend the adaptive control coordination scheme proposed in [15] to larger interconnected multi-machine electric power systems. The present paper is still taking advantage of the important features of the scheme in [15] as follows:

1. Representation of power system configuration by reduced nodal impedance matrix. In this way, any power system configuration can be represented directly and systematically. The matrix is formed only for power network nodes that have direct connections to synchronous generators. The reduced nodal impedance matrix can be derived very efficiently from the power system nodal admittance matrix and sparse matrix operations. Elements of this matrix are inputs to the neural network,

2. Representation of power system loading by active- and reactive- power of the synchronous generators. These values (available from measurements) are also inputs to the neural network, and (iii) the optimal controller parameters adaptive to system operating condition and configuration are outputs of the neural network.

However, in order to successfully apply the control coordination scheme in larger interconnected multi-machine power system environment, the present paper utilizes the following solutions and modifications to the scheme in [15]:

1. Reducing the neural network inputs number by discounting the real parts of the reduced nodal impedance matrix, given that the parameters of the transmission circuits are dominated by reactances.

2. Reducing the neural network outputs number by adapting only the controller gains to the prevailing system condition, and keep the controller time constants at the constant values. This modification is possible because the controller gains are more sensitive to system changes than the time constants [15]. By applying the above modifications, the size of the modified neural network and its training can be greatly simplified and kept to be minimal.

The application of the above two modifications are the main contributions of the present paper. Also, in the present paper, the modified neural network scheme is trained and tested with a wide range of credible power system operating conditions and configurations. For all of the tests considered, the controller parameters obtained from the trained neural network are verified by both eigenvalue calculations and time-domain simulations, which confirm that good dampings of the rotor modes are achieved, and the decrease in system dynamic performances arising from the use of fixed-parameter (non-adaptive) controllers will be removed

2. Research Method

2.1. Power System Stabilizer (PSS)

Figure 1 shows the general structure of a PSS [16] which is adopted in this paper. The structure consists of a gain block, a washout, lead-lag blocks and a limiter. A washout term/filter (i.e. with a time derivative operator) in the PSS structure is needed to guarantee that the PSS responds only to disturbances, and does not respond to any steady-state condition, when speed or power is input.

In the present work, the machine rotor speed is used for the PSS input. The PSS output is added to the exciter voltage error signal of the synchronous machine and served as a supplementary signal to add to the system damping.

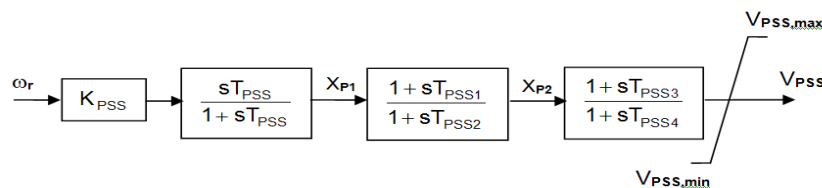


Figure 1. PSS control block diagram

2.2. Development of Neural Network-Based Stabilizer

2.2.1. General Concept of Neural Network

The relationship among the optimal controller (PSSs) parameters and power system operating condition including system configuration is, in general, a nonlinear one. The present paper draws on the key property of the multilayer feedforward neural network, which is that of nonlinear multi-variable function representation [17]. The neural network is used for the mapping between the power system configurations and/or operating conditions and optimal controller parameters.

Figure 2 is shown the general structure of the multilayer feedforward neural network which is adopted to represent the nonlinear relationship between the optimal controller parameters and power system operating condition together with configuration. There are two separate sets of nodes in the inputs layer in Figure 2. The first set has n nodes the inputs to which are obtained from the real and imaginary parts of the reduced nodal impedance matrix. These inputs represent power system configuration. If there are N_g generator nodes, the number of input nodes in the first set is $N_g^2 + N_g$, when the symmetry in the nodal impedance matrix is exploited. The second set of inputs comprises active- and reactive-power of each and every generator. There will be $2N_g$ input nodes in the second set. These inputs will represent power system operating condition. Therefore, the total number of inputs is $N_g^2 + 3N_g$. If the real parts of the reduced nodal impedance matrix are discounted, then the total number of inputs will be $0.5N_g^2 + 2.5N_g$.

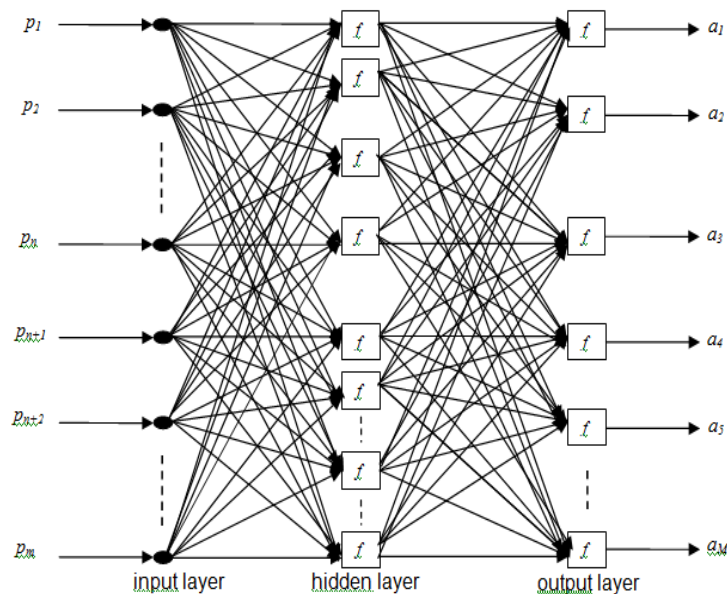


Figure 2. Structure of the neural network

The nodes in the output layer of the neural network structure in Figure 2 give the optimal values of the parameters of PSSs. The structure in Figure 2 assumes that there are M controller parameters to be tuned online. On this basis and with the controller in Figure 1, the number of output parameters from the neural network in Figure 2 is $6N_c$, where N_c is the number of PSSs. If only the PSS gains are to be tuned online, than the number of output parameters will be N_c .

The number of hidden layers, the number of nodes in each hidden layer and the weighting coefficients of the connections between nodes in the structure of Figure 2 are to be determined by neural network training, and verified by testing which will be discussed in Sections 2.2.3 and 2.2.4.

2.2.2. Overall Structure

In Figure 3 is shown the overall structure of which the neural adaptive controller described in Section 2.2.1 is a part. For online tuning of the parameters of PSSs, the inputs required are as follows:

1. Circuit-breaker and isolator status data
2. Power network branch parameters
3. Generator active- and reactive-power

The response of the trained neural network gives the optimal parameters for the PSSs. The feedback inputs to these controllers are generator speeds, as in the case of fixed-parameter controllers.

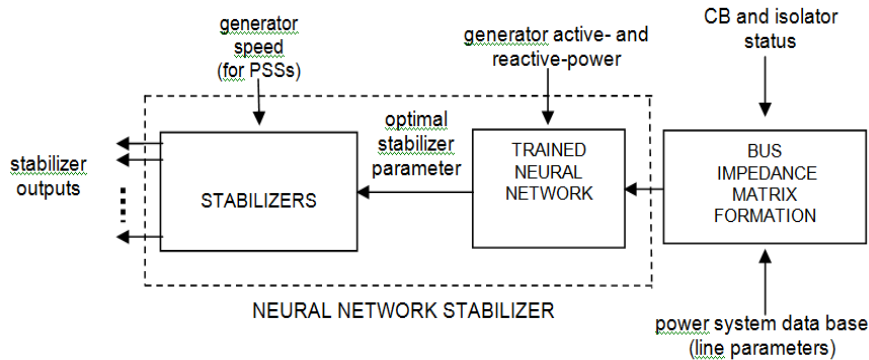


Figure 3. Neural network-based stabilizer

2.2.3. Training Procedure for Neural Network-Based Stabilizer

The training set is generated using the optimisation-based control coordination method in [4]. A brief description of the method is given in the following.

The method is based on a constrained optimisation in which the objective function formed from the real part of eigenvalues of selected modes is minimised. The method does not require any special eigenvalue/eigenvector calculation software. Eigenvalue-eigenvector equations are represented in terms of equality constraints in the optimisation. Based on the linear independence of eigenvectors, additional equality constraints are derived and included in the optimisation to guarantee distinct modes at the convergence. Inequality constraints related to minimum damping ratios required and controller parameter limits are represented in the control coordination.

For a given power system, a wide range of credible operating conditions and configurations which include those arise from contingencies is considered in the training data generation. For the i^{th} training case, the pair of specified input and output vectors is $\{p_i, t_i\}$. Based on the structure in Figure 2, the input vector p_i is:

$$p_i^T = (p_{1i}, p_{2i}, \dots, p_{mi}); i = 1, 2, \dots, N \quad (1)$$

In which N is the total number of training cases.

The target output vector t_i for the i^{th} training case is the optimal controller parameters vector for the power system with the operating condition and configuration specified by the input vector p_i .

The requirement in the training is to minimise the difference between the target output vector t_i and response of the neural network in Figure 2. For N training cases, it is proposed to minimise the following mean square error (MSE):

$$F(x) = \frac{1}{N} \sum_{i=1}^N (t_i - a_i)^T (t_i - a_i) \quad (2)$$

In (2), \mathbf{a}_i is the neural network response which has the following form, based on the structure in Figure 2:

$$\mathbf{a}_i^T = (a_{1i}, a_{2i}, \dots, a_{Mi}); i = 1, 2, \dots, N \tag{3}$$

Vector \mathbf{x} in (2) is the vector of weighting coefficients of the connections in the neural network to be identified. Minimising the error function $F(\mathbf{x})$ with respect to \mathbf{x} gives the weighting coefficient vector. In the present work, the Levenberg-Marquardt algorithm which is a second-order method with a powerful convergence property is adopted for minimising $F(\mathbf{x})$ in (2). One of the criteria for the convergence in training is that the error function $F(\mathbf{x})$ has to be less than a specified tolerance.

In addition to the training performance expressed in terms of error function $F(\mathbf{x})$, the controller parameters obtained from the trained neural network are also used for calculating the damping ratios of the rotor modes, which are then compared with the optimal damping ratios obtained at the stage of training data generation. The convergence in training is confirmed when both the error function $F(\mathbf{x})$ and the damping ratio comparison satisfy the specified tolerances.

2.2.4. Neural Network Testing and Sizing

In addition to forming the training data set, a separate testing data set is also required. The procedure for testing data generation is similar to that of training where the optimization-based control coordination method in [4] is used.

The trained neural network in Section 2.2.3 is then tested with the testing data set. The interaction among the training, testing and sizing the neural network is explained in the flowchart of Figure 4.

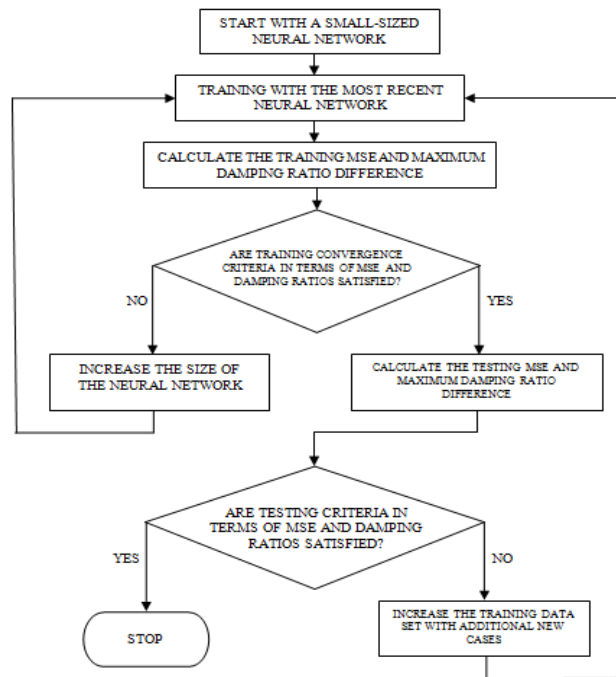


Figure 4 Flowchart for training, testing and sizing of the neural network

3. Results and Analysis

3.1. Power System Structure

The system in the study is based on the 10-machine 40-node power system of Figure 5 [18]. Initial investigation, where the damping controllers (PSSs) are not included in the system, has been carried out to determine the system oscillation damping without the controllers. Modal

analysis used in the investigation shows that there are nine electromechanical modes of oscillations.

The investigation also confirms that the system has poor damping. This low system damping indicates poor system dynamic performance and stability. Stabilization measure is, then, required for improving the damping of the oscillations. Therefore, in order to improve the stability, it is proposed to install PSSs in the system (each generator is equipped with PSS).

3.2. Design of the Neural Network-Based Stabilizer

3.2.1. Neural Network Training and Test Data

The key requirement is to design a neural controller that has the capability of generalizing with high accuracy from the training cases. This requirement is achieved through the neural network training, testing and sizing referred to in Sections 2.2.3 and 2.2.4 based on the selection of the training and testing data sets. The neural network training set should be representative of the cases described by credible system contingencies and changes in system operating conditions.

The possible contingencies of the system in Figure 5 for line outages and load variations are shown in Table 1 and 2 respectively. The input and output pairs for neural network training and testing cases are generated from the combinations of these contingencies and operating conditions.

For the system in Figure 5, the number of neural network inputs, as determined on the basis of Section 2.2.1, is 75. As mentioned also in Section 2.2.1, in order to simplify the neural network training and testing, only the controller gains are to be tuned online. Therefore, 10 linear neurons are needed in the output layer (1 for each PSS controller).

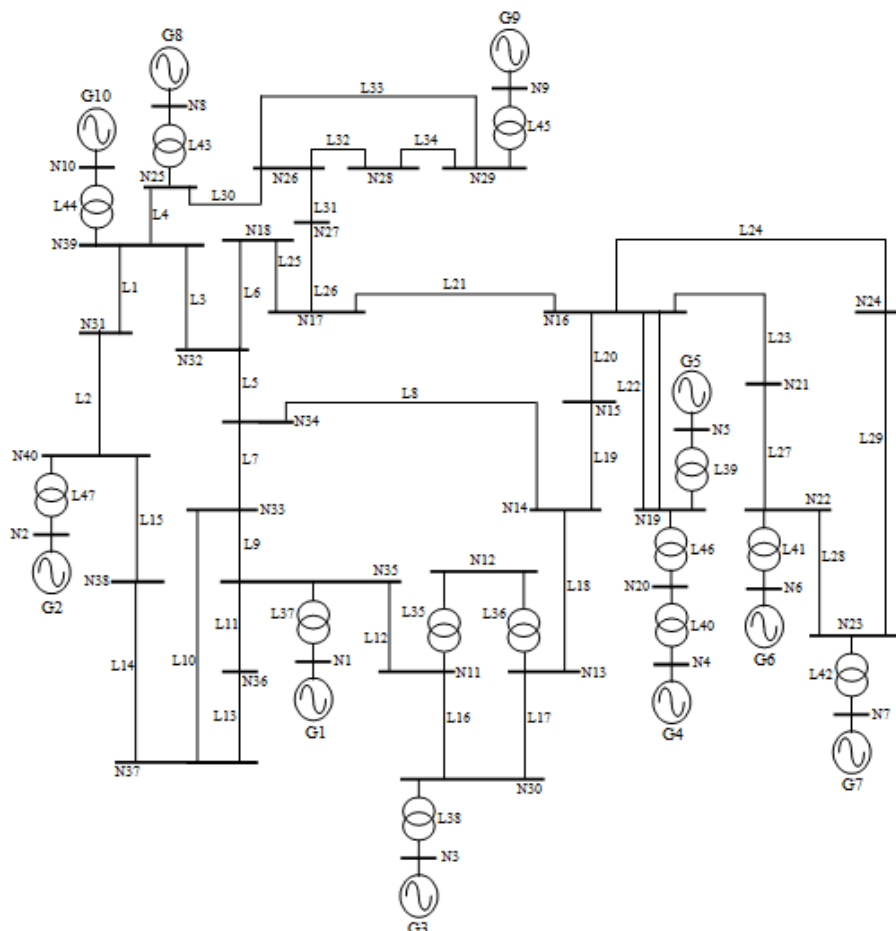


Figure 5. 10-machine 40-node power system

Table 1. Line Outages Cases

No.	Line	No.	Line	No.	Line
1.1	L1	1.13	L13	1.24	L24
1.2	L2	1.14	L14	1.25	L25
1.3	L3	1.15	L15	1.26	L26
1.4	L4	1.16	L16	1.27	L27
1.5	L5	1.17	L17	1.28	L28
1.6	L6	1.18	L18	1.29	L29
1.7	L7	1.19	L19	1.30	L30
1.8	L8	1.20	L20	1.31	L31
1.9	L9	1.21	L21	1.32	L32
1.10	L10	1.22	L22	1.33	L33
1.11	L11	1.23	L23	1.34	L34
1.12	L12				

Table 2. Variations of Load

No.	Load Demand at All Nodes	No.	Load Demand at All Nodes
2.1	50% of Base Load	2.12	105% of Base Load
2.2	55% of Base Load	2.13	110% of Base Load
2.3	60% of Base Load	2.14	115% of Base Load
2.4	65% of Base Load	2.15	120% of Base Load
2.5	70% of Base Load	2.16	125% of Base Load
2.6	75% of Base Load	2.17	130% of Base Load
2.7	80% of Base Load	2.18	135% of Base Load
2.8	85% of Base Load	2.19	140% of Base Load
2.9	90% of Base Load	2.20	145% of Base Load
2.10	95% of Base Load	2.21	150% of Base Load
2.11	100% of Base Load		

The load demands in the system are varied in the representative range between minimum and maximum values. It has been taken that the load demands at all nodes follow similar patterns. However, any different patterns of load demand variations, for example, in areas with different time zones, when they arise, can be included in the data set without difficulty.

For each contingency, the reduced nodal impedance matrix for the generator nodes 1-10 (including the slack bus) is formed. The power generations including those at the slack bus and the reactive-power which are obtained from load-flow studies and the elements of the reduced nodal impedance matrix are used as the neural network input data. The optimal controller parameters are also determined for each case using the method described in [4]. These optimal controller parameter values are used as the specified network output data.

In applying the optimal control coordination [4] for training and test data generation, the sum of the squares of the real parts of all of the eigenvalues of the electromechanical modes is maximised, with the constraints that the minimum damping ratio of the electromechanical modes is 0.1. The minimum value of 0.1 is chosen because, as mentioned also in [19, 20], the damping ratio lower than 0.1 is considered unacceptable.

The cases generated from Table 1 and 2 are sub-divided into the training set and test set. For the training set, line outage cases 1.1 – 1.3, 1.5 – 1.16, 1.18 – 1.30, and 1.32 – 1.34 together with load demand variations in cases 2.2 – 2.10, and 2.12 – 2.20 are selected. The remaining cases of line outages and load demand variations in Tables 2 and 3 are used for the test set

3.2.2. Training, Testing and Sizing the Neural Network

In the present work, the neural network is initially assumed to have one hidden layer and the number of hidden nodes is taken to be 5. The size of the neural network is then adjusted according to the procedure described in Section 2.2.4.

The performance goals specified in terms of error function $F(\mathbf{x})$ of 0.004 (for training) and 0.006 (for testing) are used. The maximum differences between the optimal damping ratio and the damping ratio calculated using neural network outputs of 0.03 (for training) and 0.05 (for testing) are also used as the performance goals. Maximum number of epoch of 100 is specified for the network training. Several network sizes (i.e. number of hidden neurons) are investigated to achieve the performance goals. Based on the investigation, it is found that the network with

10 hidden neurons in one hidden layer satisfies the convergence criteria. On this basis, the trained and tested neural network is used in the application mode, and its dynamic performance is evaluated by simulation in the following sections

3.3. Dynamic Performance of the System in the Study

Table 3 shows the comparison of modal response characteristics (electromechanical mode eigenvalues, frequencies and damping ratios) between non-adaptive (fixed-parameter) and adaptive (neural network-based) controllers of the system in Figure 5 for a range of contingencies and operating conditions. For non-adaptive controller, the controller parameters derived from the base case design are used for all of the contingency cases and load changes. It is to be noted that, as the system in Figure 5 has 9 electromechanical modes, only three modes with the lowest damping ratios are taken and shown for the comparison.

The base case (referred to as case 1 in Table 3) is that with the full system (no line outages) in Figure 5, and load demands at all nodes are at their base load values. The comparison in Table 3 for case 1 confirms that the damping ratios for the electromechanical modes achieved by the neural adaptive controller are closely similar to those obtained from the fixed-parameter controllers (i.e. non-adaptive) designed with the system configuration and operating condition specified in the base case.

Table 3. Dynamic Performances of Controllers

No	Case	Non-Adaptive Controller [4]			Adaptive Controller		
		Eigenvalues (pu)	Freq. (Hz)	Damp. Ratio	Eigenvalues (pu)	Freq. (Hz)	Damp. Ratio
1	Base Case	-1.2390 ± j11.1349	1.77	0.11	-1.2401 ± j11.1477	1.17	0.11
		-0.9672 ± j9.0460	1.44	0.11	-0.9831 ± j9.0753	1.44	0.11
		0.8482 ± j8.3001	1.32	0.10	-0.8687 ± j8.3148	1.32	0.10
2	System Load: 150% of Base Load	-1.0776 ± j11.7520	1.87	0.09	-1.1923 ± j11.8441	1.89	0.10
		-1.1584 ± j11.7529	1.77	0.10	-1.2093 ± j11.7463	1.87	0.10
		-0.6209 ± j9.6381	1.53	0.06	-0.9862 ± j10.2434	1.63	0.10
3	System Load: 140% of Base Load	-1.1191 ± j11.6405	1.85	0.10	-1.1359 ± j11.5581	1.84	0.10
		-1.2015 ± j11.6575	1.86	0.10	-1.2327 ± j11.4346	1.82	0.11
		-0.7120 ± j9.4949	1.51	0.07	-1.0067 ± j10.0525	1.60	0.10
4	Line L4 Out	-1.2377 ± j11.1359	1.77	0.11	-1.3023 ± j11.1006	1.77	0.12
		-0.9618 ± j9.0562	1.44	0.11	-1.1612 ± j10.8826	1.73	0.11
		-0.5993 ± j8.2917	1.32	0.07	-0.8284 ± j8.4445	1.34	0.10
5	Line L34 Out	-1.2375 ± j11.1368	1.77	0.11	-1.2219 ± j11.1043	1.77	0.11
		-0.9594 ± j9.0604	1.44	0.11	-0.9916 ± j9.1219	1.45	0.11
		-0.7685 ± j8.3336	1.33	0.09	-0.8462 ± j8.3497	1.33	0.10

In cases 2 and 3 of Table 3, the load demands at all nodes increase to 150% and 140% of base load respectively while the system configuration remains as that of the base case. With non-adaptive controllers, the damping ratios of the electromechanical modes decrease noticeably in comparison with those in the base case (there are modes with unacceptable damping ratios or lower than 0.1). However, with the neural adaptive controller, the damping ratios are maintained at the levels similar to those of the base case.

Further comparison in cases 4 and 5 of Table 3 focuses on contingencies where one transmission circuit is disconnected. The load demands are those in the base case. In case 4 where there is an outage of transmission line L4 in Figure 5, there is a substantial reduction in the mode damping in comparison with the base case. The damping ratio of this mode is reduced to 0.07, compared to 0.10 in the base case. With the adaptive controller, the damping ratios of all of the electromechanical modes are almost not affected by the outage, in comparison with those in the base case, as indicated in Table 3.

The outage of transmission line L34 in case 5 of Table 3 affects the damping of the electromechanical modes marginally when the non-adaptive controllers are used. The damping ratio of 0.10 in the base case is now reduced to 0.09 in the outage case 5. The robustness of the adaptive controller in this outage case is confirmed by the results of Table 3. The controller parameters determined by the trained neural network are able to adapt to the new system configuration for maintaining the modal damping ratios at the levels similar to those in the base case.

3.4. Time-Domain Simulations

In order to further validate the performance of the neural network-based controller, time-domain simulations are carried out for the selected contingency cases (i.e. 50% load increase and line L4 outage). The time-step length of 50 ms is adopted for the simulations. The descriptions of the contingency cases and the disturbances used to initiate the transients for each case are given in Table 4.

In Figure 6 is shown the system transients following the disturbance for the first contingency case (i.e. case A). It is to be noted that for this contingency, the damping ratio of the weakest mode is 0.06 when the non-adaptive controller is used (see Table 3). As the participations of generators G1 and G3 to this mode are more dominant, then the relative speed transients between generators G1 and G3 are used in forming the responses in Figure 6. From the responses, it can be seen that, with non-adaptive controller, the system oscillation is poorly damped and takes a considerable time to reach a stable condition. With the neural network-based (adaptive) controller, the system reaches steady-state condition in 5 – 6 s subsequent to the disturbance for the contingency case considered (see Figure 6). Further comparison in terms of the transients in the torque angle of generator G1 relative to that of generator G3 are given in Figure 7. The comparison confirms the improvement in electromechanical oscillation damping when the neural network-based controller is used.

In Figure 8 and 9 are shown the relative speed transient and torque angle transient for contingency case B in Table 4 respectively. For this contingency case, results similar to contingency case A are obtained. These results also confirm the improvement in electromechanical oscillation damping when the neural network-based controller is used.

Table 4. Descriptions of Contingency Cases and Disturbances

Case	Contingency Description	Disturbance Description
A	50% sudden load increase at all nodes.	Three-phase fault near node N33 on line L10. The fault is initiated at time $t = 0.10$ s, and the fault clearing time is 0.05 s.
B	Line L4 has to be disconnected to clear the fault.	Three-phase fault near node N33 on line L10. The fault is initiated at time $t = 0.10$ s, and the fault clearing time is 0.05 s.

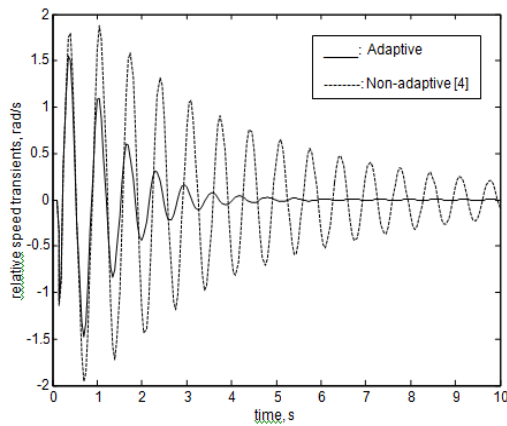


Figure 6. Relative speed (G1-G3) transients for contingency case A

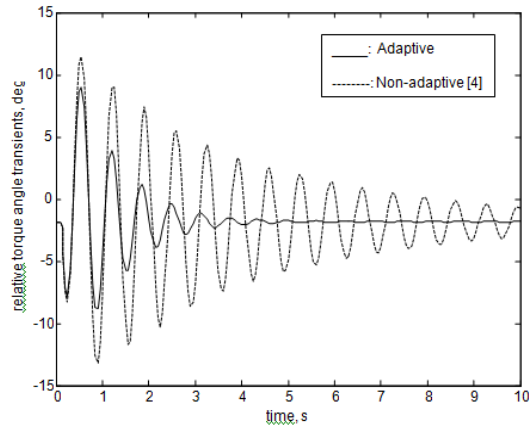


Figure 7. Relative torque angle (G1-G3) transients for contingency case A

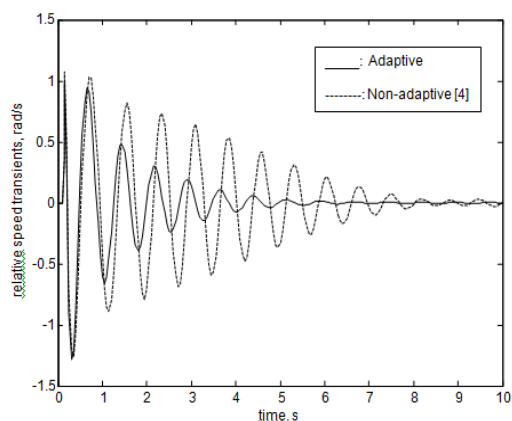


Figure 8. Relative speed (G3-G10) transients for contingency case B

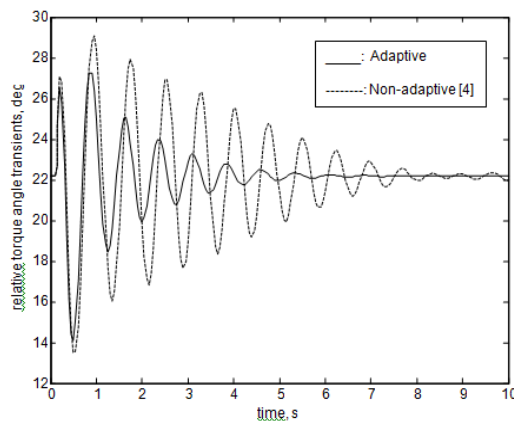


Figure 9. Relative torque angle (G3-G10) transients for contingency case B

4. Conclusion

An adaptive control algorithm and procedure have been derived and developed for online tuning of the PSSs. The procedure is based on the use of a neural network which adjusts the parameters of the controllers to achieve system stability and maintain optimal dampings as the system operating condition and/or configuration changes.

The neural network-based controller trained for a representative power system has been comprehensively tested to verify its dynamic performance. Both eigenvalue calculations and time-domain simulations are applied in the testing and verification. Many comparative studies have been carried out to quantify the improved performance of the adaptive controller in comparison with that achieved with fixed-parameter controllers. The results confirm that, by using the neural network-based controller, the decrease in system dampings and dynamic performances arising from the use of fixed-parameter controllers will be removed.

Acknowledgements

The authors would like to express special appreciation to the Ministry of Research, Technology and Higher Education (KEMENRISTEK DIKTI INDONESIA) for funding the research reported in this paper.

References

- [1] Chaudhuri B, Korba P, Pal BC. *Damping Controller Design Through Simultaneous Stabilization Technique*. Proceedings of WAC 2004. 2004; 15: 13-18.
- [2] Majumder R, Chaudhuri B, El-Zobaidi H, Pal BC, Jaimoukha IM. *LMI Approach to Normalised H-Infinity Loop-Shaping Design of Power System Damping Controllers*. IEE Proc. Gener. Transm. Distrib. 2005; 152(6): 952-960.
- [3] Nguyen TT, Gianto R. *Application of Optimization Method for Control Co-ordination of PSSs and FACTS Devices to Enhance Small-Disturbance Stability*. Proceedings of the IEEE PES 2005/2006 Transmission and Distribution Conference & Exposition. 2006: 1478-1485.
- [4] Nguyen TT, Gianto R. *Optimisation-Based Control Co-ordination of PSSs and FACTS Devices for Optimal Oscillations Damping in Multimachine Power System*. IET Gener. Transm. Distrib. 2007; 1(4): 564-573.
- [5] Nguyen TT, Gianto R. *Optimal Design for Control Coordination of PSSs and FACTS Devices with Controller Saturation Limits*. IET Gener. Transm. Distrib. 2010; 4(9): 1028-1043.
- [6] Abd-Elazim SM, Ali ES. *Optimal PSS Design in a Multimachine Power System Via Bacteria Foraging Optimization Algorithm*. WSEAS Transactions on Power Systems. 2013; 8(4): 186-196.
- [7] Ali ES. *BAT Search Algorithm for Power System Stabilizers Design in Multimachine System*. WSEAS Transactions on Power Systems. 2015; 10: 230-239.
- [8] Segal R, Kothari ML, Madhani S. *Radial Basis Function (RBF) Network Adaptive Power System Stabilizer*. IEEE Trans. Power Syst. 2000; 15(2): 722-727.

-
- [9] Liu, et al. *Adaptive Neural Network Based Power System Stabilizer Design*. IEEE Proceedings of the International Joint Conference on Neural Networks (IEEE IJCNN 2003). 2003.
- [10] Chaturvedi DK, Malik OP, Kalra PK. *Generalised Neuron-Based Adaptive Power System Stabiliser*. IEE Proc. Gener. Transm. Distrib. 2004; 151(2): 213-218.
- [11] Huma Rafi KM, Kumar P. Artificial Neural Network Based Self-Tuning Adaptive Power System Stabilizer. *International Journal of Advance Research in Science and Engineering*. 2013; 2(5): 166-175.
- [12] Memon AP, et al. Selection of Suitable Feedforward Neural Network Based PSS for Excitation Control of Synchronous Generator. *Journal Basic Appl. Sci. Res*. 2014; 4(7): 126-139.
- [13] Ginarsa IM, Zebua O. Stability Improvement of Single Machine Using ANFIS-PSS Based on Feedback-Linearization. *TELKOMNIKA*. 2014; 12(2): 315-324.
- [14] Muljono AB, Ginarsa IM, Nrartha IMA. Dynamic Stability Improvement of Multimachine Power System Using ANFIS-Based Power System Stabilizer. *TELKOMNIKA*. 2015; 13(4): 1170-1178.
- [15] Nguyen TT, Gianto R. Neural Networks for Adaptive Control Coordination of PSSs and FACTS Devices in Multimachine Power System. *IET Gener. Transm. Distrib*. 2008; 2(3): 355-372.
- [16] Mithulanathan N, Canizares CA, Reeve J, Rogers GJ. Comparison of PSS, SVC, and STATCOM Controllers for Damping Power System Oscillations. *IEEE Trans. Power System*. 2003; 16(2): 786-792.
- [17] Demuth HB, Beale M. *Neural Network Toolbox User's Guide: For Use With MATLAB (Version 4)*. The Math Works, Inc. 2004.
- [18] Pai MA. *Energy Function Analysis for Power System Stability*. Boston: Kluwer Academic Publishers. 1989.
- [19] Pourbeik P, Gibbard MJ. Simultaneous Coordination of Power System Stabilizers and FACTS Device Stabilizers in a Multimachine Power System for Enhancing Dynamic Performance. *IEEE Trans. Power Syst*. 1998; 13(2): 473-479.
- [20] Cai LJ, Erlich I. Simultaneous Coordinated Tuning of PSS and FACTS Damping Controllers in Large Power Systems. *IEEE Trans. Power Systems*. 2005; 20(1): 294-300.